Journal of Alloys and Compounds 508 (2010) 348–353

Contents lists available at ScienceDirect

Journal of Alloys and Compounds

journal homepage: www.elsevier.com/locate/jallcom

Crystal structure of $ErFe_2D_{3.1}$ and $ErFe_2H_{3.1}$ at 450 K

E.A. Sherstobitova[a,*], A. Gubkin[c], L.A. Stashkova[a], N.V. Mushnikov[a], P.B. Terent'ev[a], D. Cheptiakov[b], A.E. Teplykh[a], Junghwan Park[d,e], A.N. Pirogov[a,d]

[a] Institute of Metal Physics UD RAS, Kovalevskaya 18, 620990 Ekaterinburg, Russia
[b] Laboratory for Neutron Scattering, ETH Zürich & Paul Scherrer Institute, CH-5232 Villigen PSI, Switzerland
[c] Neutron Science Division, Korea Atomic Energy Research Institute, 305-600 Daejon, Republic of Korea
[d] Department of Physics, SungKyunKwan University, 440-746 Suwon, Republic of Korea
[e] Department of Energy Science, SungKyunKwan University, 440-746 Suwon, Republic of Korea

ARTICLE INFO

Article history:
Received 1 December 2009
Received in revised form 2 April 2010
Accepted 7 April 2010
Available online 17 September 2010

Keywords:
Metal hydride
Laves phases
Neutron diffraction

ABSTRACT

We studied crystal structure and deuterium (hydrogen) ordering in the $ErFe_2D_{3.1}$ and $ErFe_2H_{3.1}$ compounds by means of X-ray and high-resolution neutron powder diffraction at 450 K. It was found that the structure of these compounds is ascribed to the *F23* space group, which is a subgroup of the *Fd3m* group commonly applied for the RFe_2H_3-type hydrides. The deuterium and hydrogen atoms partially occupy two types of the 48h sites. Analysis of the interatomic distances allows us to assume that the occupancy factors of D (H) atoms are limited by the electrostatic repulsive interaction between the D (H) atoms.

1. Introduction

Intermetallic RFe_2 compounds easily interact with hydrogen and form hydrides RFe_2H_x with a typical hydrogen content $x \leq 4$, which are stable at room temperature [1,2]. The hydrogen penetrating into the cubic unit cell of the RFe_2 compounds causes the crystal structure transformations which can result in changes of their physical properties. Depending on the conditions of hydrogenation, hydrides of the RFe_2 compounds with a cubic, rhombohedral, orthorhombic or amorphous structure can be synthesized [4–7]. The crystalline $ErFe_2H_x$ hydrides possess the cubic structure of the C15 type for hydrogen content below $x \approx 3.2$, a rhombohedral structure for $3.2 < x < 3.7$, the C15-type structure for $x \approx 4$ at room temperature [6,8,9] and orthorhombic lattice for $x > 5$ [3]. According to the X-ray powder diffraction study [8] the $ErFe_2H_x$ compound with $x \approx 3.2$ exhibits the rhombohedral-to-cubic phase transition upon increasing temperature from 260 until 320 K. The transition was assumed to be controlled by redistribution of hydrogen atoms over the interstitial positions. The redistribution could be initiated by a spontaneous magnetoelastic rhombohedral distortion of the lattice. However, the contribution of hydrogen atoms to the X-ray diffraction scattering is negligible and, hence, there is no experimental proof for the proposed model.

The compound $ErFe_2$ is a ferrimagnet with the magnetic moment of the Fe atoms directed opposite to that of the Er atoms. The Curie temperature of $ErFe_2$ is 580 K, and the ferrimagnetic compensation temperature is 480 K [10]. Hydrogenation leads to a decrease in both the Curie and compensation temperatures [10]. According to our magnetic measurements [11], Curie temperature value of the $ErFe_3H_{3.1}$ compound is $T_C = 380$ K and the temperature dependence of magnetization shows an anomaly: the magnetization in the cubic phase is higher than that in the rhombohedral phase. A pronounced temperature hysteresis of the magnetization around the structure transition temperature indicates that the rhombohedral-to-cubic phase transition in the $ErFe_3H_{3.1}$ compound is of the first-order type.

In order to clarify the influence of hydrogen on the structural state and magnetic properties of the $ErFe_2$ compound we carried out neutron diffraction experiments in a wide temperature range from 12 K up to 450 K for the compositions, in which rhombohedral-to-cubic phase transition takes place. Along with the $ErFe_2H_{3.1}$ hydride, we prepared D-containing $ErFe_2D_{3.1}$ sample to determine localization of deuterium atoms, led by the fact that the hydrogenated compound has a large background level due to the very large incoherent scattering cross-section of hydrogen atoms reference to deuterium ones. A thorough geometrical analysis of the possible site occupations for hydrides with the *Fd3m* cubic structure of the $MgCu_2$-type is given in [12,13]. At the same time, there are only few works in which the distribution of H or D atoms over crystallographic positions has been determined experimentally [5,14,15]. In this paper we report on the crystal structure

* Corresponding author. Fax: +7 343 740003.
E-mail address: sherl@imp.uran.ru (E.A. Sherstobitova).

0925-8388/$ – see front matter © 2010 Elsevier B.V. All rights reserved.
doi:10.1016/j.jallcom.2010.04.043

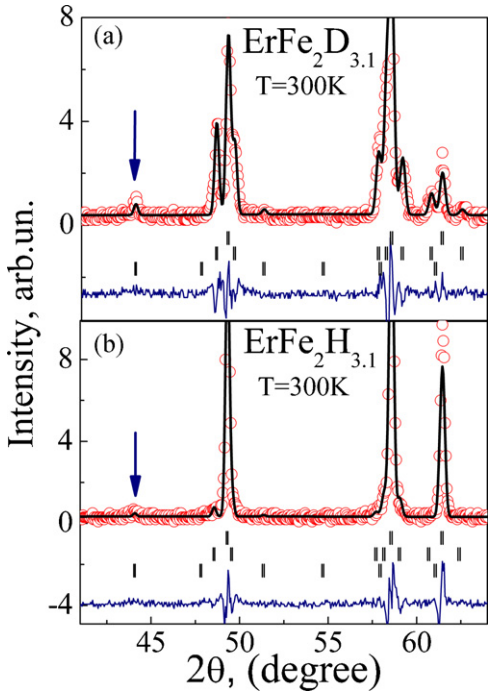

Fig. 1. Zoomed parts of XRD patterns of the $ErFe_2D_{3.1}$ (a) and $ErFe_2H_{3.1}$ (b) compounds refined in the *F23* SG at 300 K. The full line through the symbols represents the best fit. The sets of vertical marks correspond to the reflections, which can be indexed by the *F23* (upper row) and R-3m SG and impurity phase Er_2O_3 (marked by arrows).

refinement of the $ErFe_2H_{3.1}$ and $ErFe_2D_{3.1}$ compounds in the paramagnetic state at the $T = 450$ K.

2. Experimental methods

The initial $ErFe_2$ alloy has been prepared using the induction melting of the constituents in an alumina crucible under argon atmosphere and then annealed at 800 °C for 48 h. X-ray diffraction (XRD) analysis indicated that the alloy contained mainly the C15 Laves phase with the cell parameter $a = 7.273$ Å and a small amount (about, 3 wt%) of Er_2O_3 impurity phase. The hydrides were synthesized using a Sieverts-type technique. Prior to hydrogenation, the $ErFe_2$ samples were activated by heating up to 350 °C in vacuum. Absorption of hydrogen at room temperature with a gas pressure of 0.6 MPa results in the formation of the $ErFe_3H_{3.7}$ hydride. In order to reduce the hydrogen content, the samples were kept at a temperature of 88 °C and pressure of 0.05 MPa for 1 h. A similar procedure was applied to prepare deuteride. According to the gravimetric analysis, we obtained the $ErFe_3H_{3.1}$ and $ErFe_3D_{3.1}$ compositions.

XRD patterns have been measured in the temperature range 80–460 K with a DRON-type diffractometer using a monochromatized Cr Kα radiation using a home-made vacuum X-ray chamber. After heating the $ErFe_2H_{3.1}$ compound above 420 K both the *a* lattice parameter and the cell volume sharply and irreversibly decrease, which can be explained by the releasing of a part of hydrogen under heating of the sample in vacuum. According to our estimations [11], after the heating of $ErFe_2H_{3.1}$ compound up to 420 K in a vacuum the amount of stored hydrogen reduces down to $x \sim 1.6$–1.7.

Neutron powder diffraction (NPD) patterns have been recorded using the HRPT diffractometer at the PSI (Villigen, Switzerland), with a neutron wavelength of $\lambda = 1.494$ Å. In order to avoid the H or D desorption, the samples were packed into the vanadium containers under the helium atmosphere. The neutron diffraction measurements were carried out at the paramagnetic state at $T = 450$ K so as to get rid of the appearance of magnetic reflections.

The analysis of the obtained diffraction patterns has been done by means of the FullProf program [16].

3. Results and discussion

XRD patterns (Fig. 1a and b) show that the as-prepared $ErFe_2D_{3.1}$ and $ErFe_2H_{3.1}$ samples contain a mixture of the cubic and rhombohedral phases at room temperature (and a small amount 3 wt% of Er_2O_3 impurity phase). Therefore, the studied compositions are

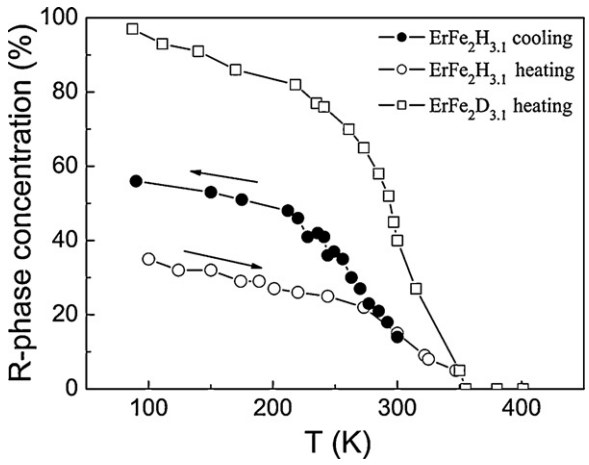

Fig. 2. Temperature dependence of the rhombohedral phase concentration in the $ErFe_2D_{3.1}$ and $ErFe_2H_{3.1}$ compounds. The lowest curve shown by open symbols was measured after fast (within 5 min) cooling of the $ErFe_2H_{3.1}$ sample down to $T = 80$ K, while the curve given by solid symbols was measured in the regime of a slow cooling within 10 h [11].

very close to the boundary line in the $ErFe_2$-H structural phase diagram [8]. It should be noted that the rhombohedral phase can be considered as a distorted cubic phase with the rhombohedral angle differing from 90° by only ~1.2°. Yet, such a distortion is sufficient to separate the diffraction lines that belong to the rhombohedral and cubic phases.

Amount of the rhombohedral and cubic phases in the compound are sensitive to temperature. Thermal variation of the relative amount of the rhombohedral phase for the $ErFe_3H_{3.1}$ and $ErFe_2D_{3.1}$ compounds is shown in Fig. 2 [11]. For both compounds, heating from liquid nitrogen temperature up to ~250 K leads to a gradual decrease in the content of the rhombohedral phase (open symbols in Fig. 2). On further temperature increase, the decreasing of the rhombohedral phase proceeds very fast, and in the temperature range from 280 to 350 K the rhombohedral-to-cubic phase transition occurs. A study of several samples with the hydrogen and deuterium content ranging from 3.05 to 3.1 revealed that the temperature ranges of the rhombohedral-to-cubic phase transition coincide for all specimens, i.e. they are single-phase with the body-centered cubic structure type above 350 K. At the same time, the amount of the rhombohedral phase at low temperatures strongly depends on the concentration *x*.

The neutron diffraction pattern analysis of $ErFe_2D_{3.1}$ sample revealed the existence of a few low intensity Bragg reflections which cannot be indexed by the *Fd3m* space group (Fig. 3a–c). These additional reflections drove us to search for another space group (SG). The SG symmetry was reduced from *Fd3m* to *F-43m*, which means the spitting of the 96g position into two 48h equivalent positions (*xxz*) type [17]. The *F-43m* symmetry allowed indexing of all low-intensity peaks however the profile line fitting was not perfect ($R_F = 5.19\%$). The SG symmetry was reduced from *F-43m* to *F23* one in which the 48h site is (*xyz*) type. All these low-intensity peaks can be fitted well within the *F23* SG ($R_F = 4.26\%$) which allows the 3 coordinates refinement (*xyz*) in comparison with 2 coordinates refinement (*xxz*) for the SG *F-43m* (Fig. 3d–f). Thus, the structure of these compounds is ascribed to the *F23* SG, which is a subgroup of the *Fd3m* SG commonly applied for the RFe_2H_3-type hydrides.

The atomic coordinates and the occupancy factors, calculated from both of *F23* and *Fd3m* SG, are given in Table 1. One can see from Table 1 that the D atoms only partially occupy both types of the 48h sites. The total content of deuterium in the compound was estimated to be $x = 3.36(4)$ using the occupation numbers (15%

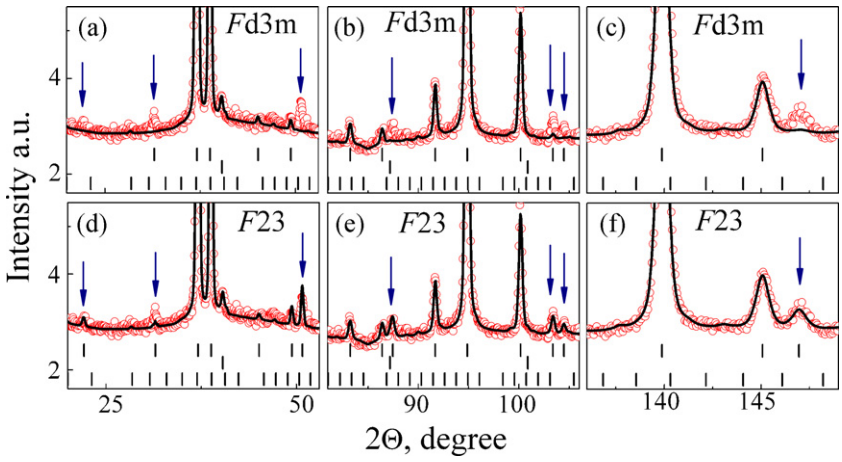

Fig. 3. Zoomed parts of NPD patterns of the $ErFe_2D_{3.1}$ compound refined in the *Fd3m* (a–c) and *F23* (d–f) SG at the temperature $T = 450$ K. The full line through the symbols represents the best fit. First row of the dashes denotes the reflections, which can be ascribed to the *Fd3m* (a–c panels) or the *F23* SG (d–f panels); the second row corresponds to the vanadium sample container; the third line corresponds to the Er_2O_3 impurity Bragg reflections. The superstructure reflections which cannot be fitted in the *Fd3m* SG are marked by the arrows.

Table 1
Atomic positions (*x*,*y*,*z*) and occupancy of $ErFe_2D_{3.1}$ at 450 K. The crystal symmetry is cubic *F23* SG with $a = 7.791(2)$ Å, $V = 473$ Å^3. Agreement factors: $R_F = 4.26\%$, $\chi^2 = 3.98$.

Atom (Wyckoff)	*x*(*δx*)	*y*(*δy*)	*z*(*δz*)	Occupancy (*δN*)
Er_1(4a)	0.000	0.000	0.000	1
Er_2(4c)	0.250	0.250	0.250	1
Fe(16e)	0.625	0.625	0.625	1
D_1(48h)	0.0435(8)	0.2672(3)	0.0531(9)	0.41(1)/D
D_2(48h)	0.7250(3)	0.9951(10)	0.7265(27)	0.15(1)/D
				D(total)/f.u. = 3.36(4)

The closest interatomic distances *d* (Å) and standard deviation *δd* (Å)

D site	d_{Er1} (Å) (*δd*)	d_{Er2} (Å) (*δd*)	d_{Fe} (Å) (*δd*)	d_{D1} (Å) (*δd*)	d_{D2} (Å) (*δd*)
D_1(48h)	2.1495(28)	2.2259(70)	1.7489(68), 1.6671(59)	1.0607(95), 2.4113(76), 2.0351(72)	
D_2(48h)	2.4852(234)	2.0036(90)	1.66671(181), 1.6849(199)	1.4263(239), 1.5351(237), 1.7702(244), 1.8454(242), 2.1659(240), 2.2099(240)	0.5294(331), 2.4231(249)

The crystal symmetry is cubic *Fd3m* SG. Agreement factors: $R_F = 6.04\%$, $\chi^2 = 10.18$

Atom (Wyckoff)	*x*(*δx*)	*y*(*δy*)	*z*(*δz*)	Occupancy (*δN*)
Er_1(8a)	0.125	0.125	0.125	1
Fe(16d)	0.500	0.500	0.500	1
D_1(96g)	0.3332(1)	0.3332(1)	0.1373(2)	0.31(1)/D
				D(total)/f.u. = 3.72(3)

The closest interatomic distances *d* (Å) and standard deviation *δd* (Å)

D site	d_{Fe} (Å) (*δd*)	d_{Fe} (Å) (*δd*)	d_{D1} (Å) (*δd*)
D_1(96g)	2.0995(10), 2.2965(12)	1.6948(13)	0.9210(13), 1.4289(14), 2.0066(13), 2.1522(18)

and 41%) which is in a reasonable agreement with the value $x = 3.1$, determined from the gravimetric measurements.

The NPD pattern of the $ErFe_3H_{3.1}$ compound has some differences in the reflection intensity if to compare it with the NPD pattern of the $ErFe_2D_{3.1}$ at 450 K (Fig. 4). Also one can notice that there are not clearly seen low-intensity superstructure reflections on the NPD pattern of the $ErFe_3H_{3.1}$ compound. It can be explained by a difference of the *b* scattering length for D and H atoms (6.6 and −3.7 fm, respectively) as well as the high background level because of large incoherent neutron scattering by the H nucleus. Nevertheless, the profile line fitting comparison for both of *Fd3m* and *F23* SG shows a better goodness of fitting and lesser agreement factor $R_F = 7.86\%$ for the *F23* SG rather than for *Fd3m* SG $R_F = 9.4\%$ (see Fig. 5, Table 2). The coordinate parameters and occupation factors for the $ErFe_3H_{3.1}$ hydride in the *F23* and *Fd3m* SG are given in Table 2. As one can see, the occupancies of the two 48h sites by H atoms in the *F23* SG are equal to 30% and 23%, respectively. The estimation of the total content of H atoms on the basis of the occupancy factors in the

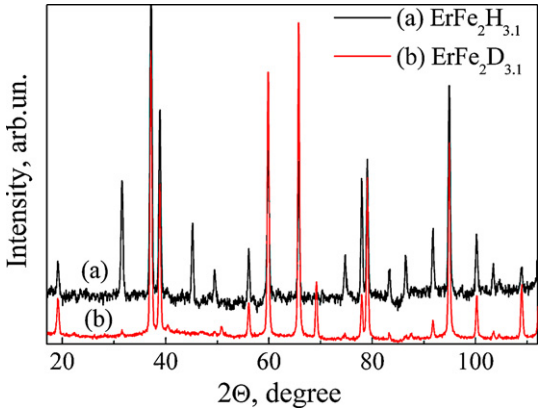

Fig. 4. NPD patterns of the $ErFe_2H_{3.1}$ (a) and $ErFe_2D_{3.1}$ (b) compounds, measured at the temperature $T = 450$ K.

Table 2
Atomic positions (*x*,*y*,*z*) and occupancy of $ErFe_2H_{3.1}$ at 450 K. The crystal symmetry is cubic *F* SG with *a* = 7.792(2) Å, *V* = 473 Å^3. Agreement factors: R_F = 7.86%, χ^2 = 2.11.

Atom (Wyckoff)	*x*(δ*x*)	*y*(δ*y*)	*z*(δ*z*)	Occupancy (δN)
Er_1(4a)	0.000	0.000	0.000	1
Er_2(4c)	0.250	0.250	0.250	1
Fe(16e)	0.625	0.625	0.625	1
D_1(48h)	0.05383(43)	0.2858(13)	0.0585(44)	0.30(1)/H
D_2(48h)	0.7650(20)	0.9932(15)	0.7926(14)	0.23(1)/H
				H(total)/f.u. = 3.18(4)

The closest interatomic distances *d* (Å) and standard deviation δ*d* (Å)

D site	d_{Er1} (Å) (δ*d*)	d_{Er2} (Å) (δ*d*)	d_{Fe} (Å) (δ*d*)	d_{H1} (Å) (δ*d*)	d_{H2} (Å) (δ*d*)
H_1(48h)	2.3128(165)	2.1509(387)	1.7226(230), 1.6759(363)	1.2466(551), 1.7386(417), 2.5275(408)	
H_2(48h)	2.4431(140)	2.0319(125)	1.5442(135), 1.7843(129)	1.3579(403), 1.5744(383), 1.6746(408), 1.9356(418), 2.1147(401), 1.3597(384)	0.7039(172), 2.5265(172)

The crystal symmetry is cubic *Fd3m* SG. Agreement factors: R_F = 9.4%, χ^2 = 2.36

Atom (Wyckoff)	*x*(δ*x*)	*y*(δ*y*)	*z*(δ*z*)	Occupancy (δ*N*)
Er_1(8a)	0.125	0.125	0.125	1
Fe(16d)	0.500	0.500	0.500	1
H(96g)	0.3388(6)	0.3388(6)	0.1434(11)	0.23(1)/H
				H(total)/f.u. = 2.83(4)

The closest interatomic distances *d* (Å) and standard deviation δ*d* (Å)

H site	d_{Er} (Å) (δ*d*)	d_{Fe} (Å) (δ*d*)	d_{H1} (Å) (δ*d*)
H_1(96g)	2.1295(48), 2.3608(69)	1.6575(59)	0.7980(66), 1.5093(72), 1.9991(70), 2.1536(98)

F23 SG gives the value *x* = 3.18(4), which is in a fair agreement with *x* = 3.1, obtained from the gravimetric data. The refinement of the $ErFe_2H_{3.1}$ compound in the *Fd3m* SG revealed that H atoms occupied only 96g sites by 23%. The total content of H atoms is estimated to be *x* = 2.83(4) which is lesser than the gravimetric value. Thus, the model *F23* SG shows the better agreement of the hydrogen content *x* with the gravimetric data.

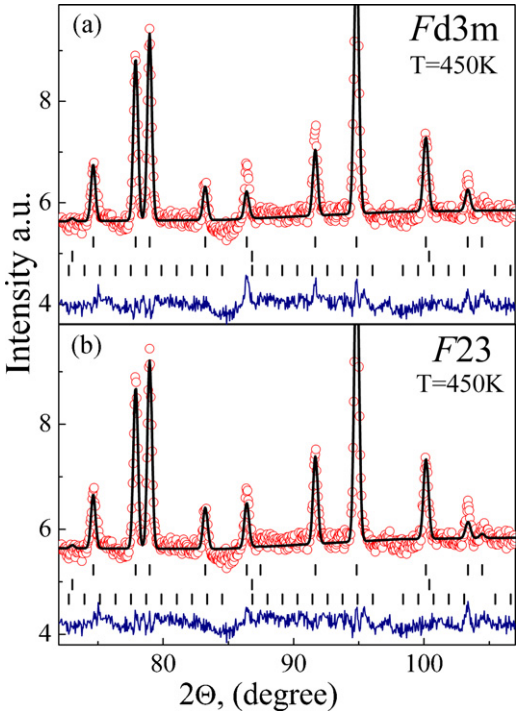

Fig. 5. Zoomed part of NPD patterns of the $ErFe_2H_{3.1}$ compound refined in the model of the *Fd3m* (a) and *F23* (b) SG at the temperature *T* = 450 K. The full line through the symbols represents the best fit. First row of the dashes denotes the reflections, which can be ascribed to (a) the *Fd3m* and (b) the *F23* SG; the second row corresponds to the vanadium sample container; the third line corresponds to the Er_2O_3 impurity Bragg reflections.

As can be seen from Tables 1 and 2, the crystal structure of the $ErFe_2H_{3.1}$ is identical with the $ErFe_2D_{3.1}$ one in terms of the model *Fd3m* SG. Fig. 6 shows the atomic projection on the *ab*-basic plane of that structure. Let us turn to the model of *F23* SG. As one can see from Tables 1 and 2, the Er and Fe atoms are located at the same positions for both compounds. However, the distribution of the H atoms over the interstitial sites for the $ErFe_2H_{3.1}$ compound is not similar to that for the $ErFe_2D_{3.1}$ compound in the *F23* SG. Moreover, the calculated occupation numbers of both 48h positions are different: 41% and 15% of the 48h sites are occupied for the $ErFe_2D_{3.1}$ compound while these occupancy factors are 30% and 23% for $ErFe_2H_{3.1}$ compound. The atomic projections on the *ab*-

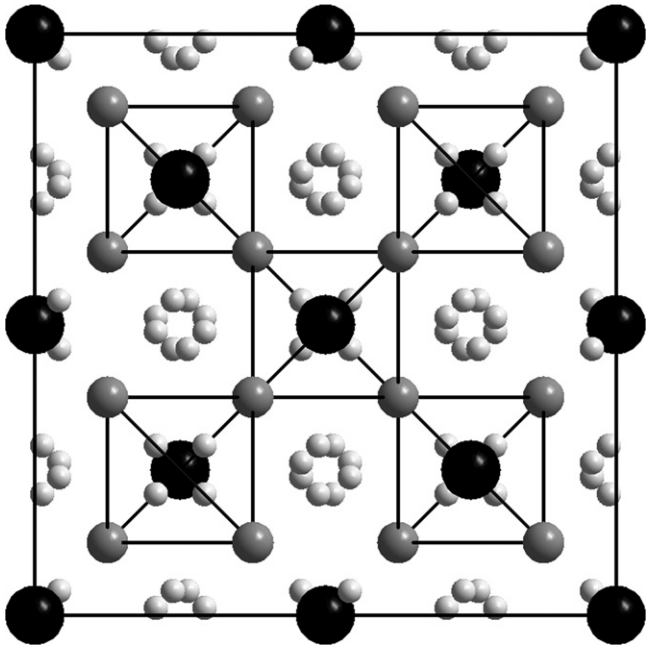

Fig. 6. Atomics projection on the *ab*-basic plane of the $ErFe_2D(H)_{3.1}$ structure, refined in the model *Fd3m* SG.

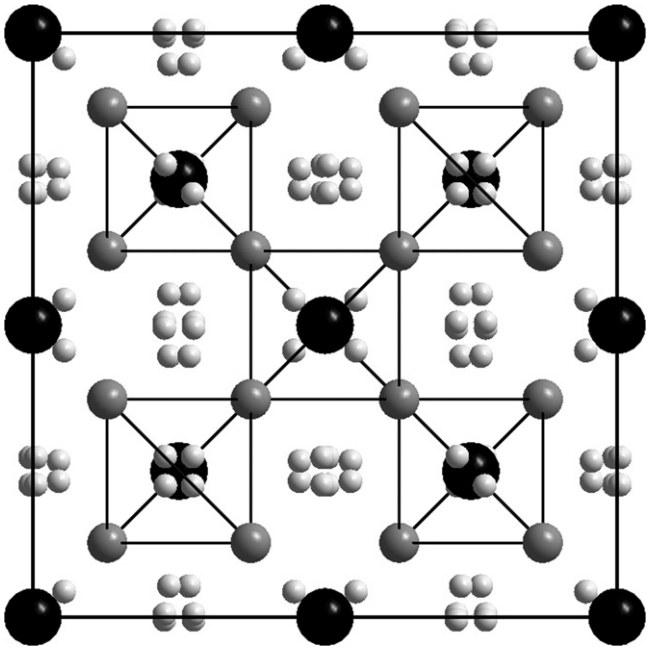

Fig. 7. Atomics projection on the *ab*-basic plane of the $ErFe_2D_{3.1}$ structure, refined in the model *F23* SG.

basic plane of the ErFe$_2$D3.1 and $ErFe_2H_{3.1}$ structure, refined from the diffraction pattern in the *F23* SG are shown in Figs. 7 and 8, respectively.

There are two possible explanations of that difference in the location of the D and the H atoms over the interstitials. The first one is so-called isotopic effect. It means the crystal structure of the $ErFe_2H(D)_{3.1}$ compound depends on the sort of a H isotope because of different H and D isotope masses. Other possible explanation is the different concentration x of the H and the D atoms in the $ErFe_2D_{3.1}$ and the $ErFe_2H_{3.1}$ compounds. According to the NPD data analysis at 450 K the total contents of the D and H atoms are estimated to be $x = 3.36(4)$ and $x = 3.18(4)$, respectively. The amount

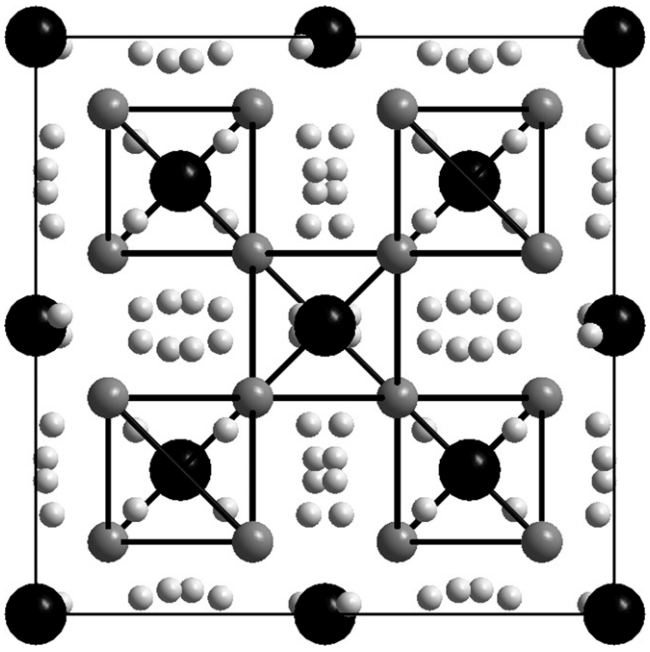

Fig. 8. Atomics projection on the *ab*-basic plane of the $ErFe_2H_{3.1}$ structure, refined in the model *F23* SG.

of the rhombohedral phase at the low temperature range strongly depends on x: it increases with increasing the D and H atoms content [11]. According to the XRD measurements at 300 K the amount of the rhombohedral phase is 40 wt% for the $ErFe_2D_{3.1}$ and 17 wt% for the $ErFe_2H_{3.1}$ (see Fig. 2). Bearing in the mind the concentration dependence of the rhombohedral phase amount we may conclude that such a difference in the 48h sites occupation by the D and H atoms can be understood in terms of different value of the deuterium and hydrogen concentration in the $ErFe_2D_{3.1}$ and $ErFe_2H_{3.1}$ compounds.

In the C15 cubic structure (*Fd3m* SG) the D (H) atoms can occupy three different types of interstitial tetrahedral sites [12,13]. At a 96g position, usually denoted as A_2B_2, the D (H) atom is surrounded by two Er and two Fe atoms. The site 32e is denoted as AB_3, where D (H) atom is surrounded by one Er and three Fe atoms. The third 8b position is a B_4 interstitial site with four Fe neighbors. The AB_3 interstitial site for the $ErFe_2H_x$ has the largest size [8], whereas the B_4 site has the smallest one. Since the D (H) atoms interact more easily with rare earth elements than with 3d-elements, the D (H) atoms prefer to occupy interstitial sites with the maximum number of surrounding RE atoms. Therefore, the hydrogen and deuterium never reside in the B_4 interstitial sites, whereas both the AB_3 and A_2B_2 sites can be filled by the D (H) atoms [6,14]. The complete filling of the AB_3 and A_2B_2 interstitials leads to the formation of the $ReFe_2H_{16}$ hydride. Such high hydrogen concentration cannot be reached, mainly because of negative electrostatic interactions of the D (H) atoms. According to the Switendick criterion [13], two hydrogen atoms cannot occupy two sites if the distance between these sites is less than 2.10 Å. Tables 1 and 2 present the interatomic distances Fe–D (H), Er–D (H) and D (H)–D (H), refined from the diffraction pattern within the *F23* SG (standard deviation of these parameters were calculated by the FullProf program). One can see that some of the D_1 (H)–D_2 (H), D_1 (H)–D_1 (H) and D_2 (H)–D_2 (H) distances are too short for these positions to be occupied by two D (H) atoms because of the repulsive interaction between the D (H) atoms. Apparently, it is the reason why the D_1 (H) and D_2 (H) sites are only partially occupied.

Using our structural data, we can suggest the following scenario of structure formation of the $ErFe_2D_{3.1}$ and $ErFe_2H_{3.1}$ compounds at 450 K. The D (H) atoms occupy only the A_2B_2 interstitial sites in the C15 structure of the parent $ErFe_2$ compound, while both the B_4 and AB_3 interstitial sites are empty. Since for the $ErFe_2D_{3.1}$ (and $ErFe_2H_{3.1}$) compositions only a part of the A_2B_2 sites is filled by the deuterium (hydrogen), the electrostatic interaction between the D (H) atoms leads to the formation of an ordered configuration within the A_2B_2 sites. The ordering causes the crystal symmetry lowering from the *Fd3m* to the *F23* SG, and the 96g site splits into two 48 h sites, which leads to the occurrence of additional weak intensity lines on the NPD patterns of the $ErFe_2D_{3.1}$ compound.

4. Conclusion

We prepared the $ErFe_2D_{3.1}$ and $ErFe_2H_{3.1}$, compounds, the composition of which is very close to the boundary line between the cubic and rhombohedral structure in the $ErFe_2$–D (H) structural phase diagram. The analysis of the NPD pattern of the $ErFe_2D_{3.1}$ compound at 450 K revealed the superstructural reflections in addition to the reflections of the parent C15 cubic structure. The crystal structure of the $ErFe_2D_{3.1}$ and $ErFe_2H_{3.1}$ compounds is identified within the *F23* SG, with deuterium (hydrogen) ordering over two types of the 48h sites. For the *F23* symmetry the positions of the D (H) atoms are not completely occupied: 41% and 15% of the 48h sites are occupied in the lattice of the $ErFe_2D_{3.1}$ while in the $ErFe_2H_{3.1}$ these occupancy factors are 30% and 23%. The fact of partial occupation is in agreement with the existence of short D (H)–D_2 (H), D_1

(H)–D_1 (H) and D_2 (H)–D_2 (H) distances, which excludes a simultaneous filling of these positions because of the repulsive interaction between the D (H) atoms. The difference in the 48h sites occupation by the H and D atoms can be explained by a small difference in deuterium and hydrogen concentration x in the $ErFe_2D_{3.1}$ and $ErFe_2H_{3.1}$ compounds.

Acknowledgements

The study is supported by the RAS Programs: "Fundamental development of energy system and technology"; project No. 13 and "Synthesis, structure and physical-chemical properties of hydrogen storage materials"; project No. 52; project No. 09-T-2-1012. Neutron diffraction experiment was supported by the SCOPES I B7420-110849 and Program of UD of RAS, project No. 24.

References

[1] W.E. Wallace, in: G. Alefeld, J. Völkl (Eds.), Hydrogen in Metal 1. Basic Properties, vol. 28, Springer-Verlag, Berlin, 1978, pp. 169–201.
[2] G. Wiesinger, G. Hilscher, in: K.H.J. Buschow (Ed.), Handbook of Magnetic Materials, vol. 17, Elsevier, Amsterdam, 2008, pp. 293–456.
[3] H. Sugiura, I. Marchuk, V. Paul-Boncour, A. Percheron-Guégan, T. Kitazawa, S.M. Filipek, J. Alloys Compd. 356–357 (2003) 32–35.
[4] K.H.J. Buschow, Phys. B+C 79 (1977) 86–88.
[5] A.V. Andreev, A.V. Deryagin, V.N. Moskalev, N.V. Mushnikov, Phys. Status Solidi A 73 (1982) K69–K71.
[6] D. Fruchart, Y. Berthier, T. de Saxce, P.J. Vulliet, J. Less-Common Met. 130 (1987) 89–96.
[7] K. Aoki, T.J. Masumoto, J. Alloys Compd. 194 (1993) 251–261.
[8] A.V. Andreev, A.V. Deryagin, A.A. Yezov, N.V. Mushnikov, Phys. Metall. Metallogr. 58 (1984) 124–128.
[9] K. Shashikala, P. Raj, A. Sathyamoorthy, Mater. Res. Bull. 31 (1996) 957–963.
[10] A.V. Deryagin, N.V. Kudrevatykh, V.N. Moskalev, N.V. Mushnikov, Phys. Metall. Metallogr. 58 (1984) 96–100.
[11] L.A. Shreder, V.S. Gaviko, N.V. Mushnikov, P.B. Terent'ev, Solid State Phenom. 152–153 (2009) 33–36.
[12] D.P. Shoemaker, C.B. Shoemaker, J. Less-Common Met. 68 (1979) 43–58.
[13] D.G. Westlake, J. Less-Common Met. 90 (1983) 251–273.
[14] V. Paul-Boncour, S.M. Filipek, I. Marchuk, G. André, F. Bourée, G. Wiesinger, A. Percheron-Guégan, J. Phys.: Condens. Matter. 15 (2003) 4349–4359.
[15] G. Wiesinger, V. Paul-Boncour, S.M. Filipek, Ch. Reichl, I. Marchuk, A. Percheron-Guegan, J. Phys.: Condens. Matter. 17 (2005) 898–908.
[16] J. Rodriguez-Carvajal, Phys. B 192 (1993) 55–69.
[17] Th. Hahn (Ed.), International Tables for Crystallography, Vol. A: Space-Group Symmetry, 4th revised ed., Kluwer Academic Publishers, Dordrecht, 1995.